Available online at www.sciencedirect.com

ScienceDirect

IFAC Papers Online CONFERENCE PAPER ARCHIVE

IFAC-PapersOnLine 48-1 (2015) 604–609

Modeling the Dynamics of a Flexible Belt Drive Using the Equations of a Deformable String with Discontinuities

Yu. Vetyukov * **V. Eliseev** ** **M. Krommer** ***

* *Johannes Kepler University Linz, Institute of Technical Mechanics, Altenbergerstr. 69, 4040 Linz, Austria (e-mail: yury.vetyukov@jku.at)*
** *St. Petersburg State Polytechnical University, Faculty of Mechanics and Mechanical Engineering, Polytechnicheskaya ul. 29, 195251 St. Petersburg, Russia (e-mail: yeliseyev@inbox.ru)*
*** *Vienna University of Technology, Institute of Mechanics and Mechatronics, Karlsplatz 13, 1040 Vienna (e-mail: michael.krommer@tuwien.ac.at)*

Abstract: The transient analysis of a belt drive is based on a nonlinear dynamic model of an extensible string at contour motion, in which the trajectories of particles of the belt are predetermined. The equations of string dynamics at the free spans are considered in a fixed domain by transforming into a spatial frame. Assuming the absence of slip of the belt on the surface of the pulleys, we arrive at a new model with a discontinuous velocity field and concentrated contact forces. Finite difference discretization allows numerical analysis of the resulting system of partial differential equations with delays. Example solution for the case of start up and accelerated motion of a friction belt drive is presented and discussed.

Keywords: Axially moving structures, Eulerian description, Partial differential equations, Delay differential equations, Finite differences

1. INTRODUCTION

In the present paper we numerically study transient dynamics of a belt drive based on the model, which has earlier been presented by the authors in (Eliseev, 2009; Eliseev and Vetyukov, 2012; Vetyukov and Eliseev, 2014). Velocity and strain of the extensible belt vary between the tight and the slack sides of the drive, which leads to the sliding friction between the belt and the pulleys. This model of creep of the belt near the points, where it leaves the pulleys, was first studied by Reynolds (1874) and is adopted in the engineering and technical literature, see e.g. Niemann and Winter (1986); Stolarski (1990); Brar and Bansal (2004). Common assumptions ignore dynamic effects due to the acceleration of the belt; other hypotheses concerning redistribution of tension forces between the tight and the slack sides of the drive are often involved.

In the framework of the creep theory, Rubin (2000) and Bechtel et al. (2000) used a model of extensible string for describing steady operation of a belt drive. Solving the equations of string mechanics (Antman, 1995) for the case of steady motion (see e.g. Nordenholz and O'Reilly (1995)), Rubin (2000) consistently analyzes the fields of velocity and strain of the belt in three qualitatively different domains: at the free spans, at the zones of perfect contact between the belt and the pulley, as well as at the zones of sliding friction contact. Resulting relations for the rotational moments at the pulleys, their angular velocities and coefficient of efficiency of the belt drive are shown to be different from the results in the technical literature. For further extensions to viscoelastic behavior of the belt see Morimoto and Iizuka (2012); to a non-classical friction law between the belt and the pulley see Kim et al. (2011); to a rod model of the belt with bending stiffness see Kong and Parker (2005). Small deviations from a steady motion were studied by Leamy (2005) using perturbation techniques.

Eliseev (2009) suggested a novel approach to analyzing an extensible belt, whose particles are moving along a given contour. In section 2 of this paper we transform the equations of nonlinear string dynamics to spatial (Eulerian) description. The resulting system of equations in a domain with fixed boundaries is applicable to the analysis of unsteady operation of the drive.

We assume perfect contact of the belt with the pulleys, similar to a synchronous drive with a timing (toothed) belt. In the present paper we apply this idealized model to a friction drive, which shall be considered as a limiting case of the above mentioned creep model when the zone of slip degenerates to a point. This allows for a relatively simple treatment of unsteady regimes of motion in both numerical and analytical contexts. As a consequence, contact forces between the pulley and the belt are concentrated in points, and discontinuities in the velocity and strain of the belt need to be treated. The corresponding jump conditions are new for the analysis of belt drives dynamics; see Irschik (2007) for general relations of jump of mass and

⋆ Support of Yury Vetyukov from the Austrian COMET-K2 programme of the Linz Center of Mechatronics (LCM) is gratefully acknowledged.

10.1016/j.ifacol.2015.05.097

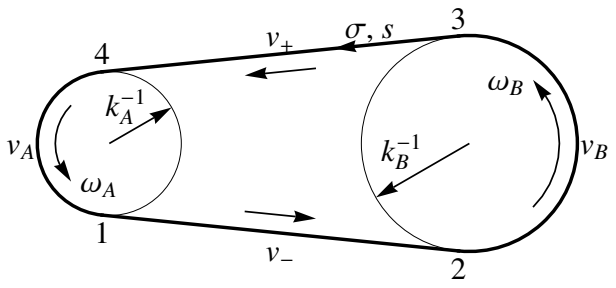

Fig. 1. Scheme of a two-pulley drive with the domains of motion of the belt: 12, 34 – straight free spans (slack span and tight span respectively), 41, 23 – regions of contact with the driving pulley A and with the driven one B; the single arc coordinate σ is counted from the point 4; s is the material coordinate

momentum. The range of applicability of this idealized contact model to real structures is yet to be justified in the future work.

In section 3 of the present work we shortly recall the results of the analysis of steady operation of belt drives, presented by the authors in (Eliseev and Vetyukov, 2012). The benefits of the spatial description and of the idealized model of belt-pulley contact are demonstrated in section 4, in which we outline a strategy for simple and consistent transient analysis, earlier presented in (Vetyukov and Eliseev, 2014). Subsequent sections of the paper present a novel numerical scheme for the solution of the system of partial differential equations with delays in the boundary conditions. Based on the finite difference discretization with respect to the spatial variable, the scheme has been implemented in *Wolfram Mathematica* [1] environment, which was proven to be efficient for numerical modeling of problems of structural mechanics (Vetyukov, 2014).

2. EQUATIONS OF BELT DYNAMICS AT CONTOUR MOTION

A two-pulley belt drive is schematically presented in Fig. 1. At contour motion, the material points of the belt follow the trajectory, which is plotted by a thick line. The material particles travel across the boundaries of the contact regions 1…4. This makes spatial description of the dynamics of the belt as an extensible string advantageous in the present case. In this section we recall and revise the equations of string dynamics, which were derived in (Eliseev and Vetyukov, 2012).

The considered trajectory can be parametrically specified by the dependence of the position vector $\boldsymbol{R}$ on the arc coordinate σ with the following geometrical relations:

$$\boldsymbol{R} = \boldsymbol{R}(\sigma), \quad \boldsymbol{R}'(\sigma) = \boldsymbol{\tau}, \quad \boldsymbol{\tau}'(\sigma) = k\boldsymbol{n}, \tag{1}$$

in which $k(\sigma)$ is the curvature, $\boldsymbol{\tau}$ is the unit tangent vector and $\boldsymbol{n}$ is the unit vector of normal to the trajectory. In Fig. 1 the contour coordinate is looped, and the values $\sigma = 0$ and $\sigma = \sigma_4$ correspond to the same point 4. The domains $0 \le \sigma \le \sigma_1$ and $\sigma_2 \le \sigma \le \sigma_3$ answer respectively to the driving pulley A with $k = k_A$ and the driven one B with $k = k_B$. The slack span $\sigma_1 \le \sigma \le \sigma_2$ and the tight one $\sigma_3 \le \sigma \le \sigma_4$ are straight with $k = 0$.

[1] http://www.wolfram.com

At spatial description, our aim is to find the variation of the material coordinate s of the string for a given point in space over the time t:

$$s = S(\sigma, t). \tag{2}$$

In the reference configuration $s = S(\sigma, 0) = \sigma$. Stretch of the string equals to $\partial\sigma/\partial s \equiv \partial_s\sigma$, and the strain measure is expressed using the rule for an inverse function:

$$\varepsilon = \partial_s\sigma - 1 = (S')^{-1} - 1; \tag{3}$$

we denote the derivative with respect to the spatial coordinate σ with a prime. The tension force Q is related to the strain by a linear constitutive law

$$Q = Q_0 + b\varepsilon, \tag{4}$$

in which Q_0 is the tension in the reference configuration (pre-tension) and b is the stiffness of the belt.

The velocity of a particle of the belt is the material time derivative

$$\boldsymbol{v} = \partial_t\boldsymbol{R} = v\boldsymbol{\tau}, \quad v \equiv \partial_t\sigma, \quad \partial_t(\cdots) \equiv \left.\frac{\partial\cdots}{\partial t}\right|_{s=\text{const}}. \tag{5}$$

Transforming to the spatial description, we find

$$0 = \partial_t s = vS' + \dot{S} \quad \Rightarrow \quad v(\sigma, t) = -\dot{S}(S')^{-1}, \tag{6}$$

in which the derivative with respect to time t at a given point in space $\sigma = \text{const}$ is denoted with a dot.

The equation of balance of forces (Antman, 1995)

$$\partial_s\left(Q\boldsymbol{\tau}\right) + \boldsymbol{q} = \rho\boldsymbol{w} \tag{7}$$

features the vector of the external force $\boldsymbol{q}$ and mass ρ per unit length of the belt in the reference configuration $\mathrm{d}s$. At spatial description, components of the vector of acceleration $\boldsymbol{w} \equiv \partial_t\boldsymbol{v}$ take the form

$$w_\tau = vv' + \dot{v}, \quad w_n = kv^2, \quad \boldsymbol{w} = w_\tau\boldsymbol{\tau} + w_n\boldsymbol{n}. \tag{8}$$

Introducing the force factor $\tilde{\boldsymbol{q}}$ and belt density m per unit length of the contour in space $\mathrm{d}\sigma$ according to

$$\tilde{\boldsymbol{q}} \equiv \boldsymbol{q}S', \quad m \equiv \rho S' \tag{9}$$

and projecting onto the local basis vectors $\boldsymbol{\tau}$ and $\boldsymbol{n}$, we rewrite the equations of balance (7) in a spatial form:

$$\begin{aligned} Q' + \tilde{q}_\tau &= mw_\tau, \\ kQ + \tilde{q}_n &= mw_n. \end{aligned} \tag{10}$$

Equation of balance of mass at spatial description reads

$$\int_{s_1}^{s_2} \rho\,\mathrm{d}s = \int_{\sigma_1}^{\sigma_2} m\,\mathrm{d}\sigma \quad \Rightarrow \quad \dot{m} + (mv)' = 0. \tag{11}$$

At the driven pulley with the radius k_B^{-1} the loading moment $M_B(t)$ is computed as follows:

$$M_B = -k_B^{-1}\int_{S(\sigma_2,t)}^{S(\sigma_3,t)} q_\tau\,\mathrm{d}s = -k_B^{-1}\int_{\sigma_2}^{\sigma_3} \tilde{q}_\tau\,\mathrm{d}\sigma. \tag{12}$$

3. STEADY OPERATION

In a steady regime the velocity, force and strain at a given point in space do not change in time. We have $v = v(\sigma)$, $Q = Q(\sigma)$, $\varepsilon = \varepsilon(\sigma)$, and from (3) it follows that

$$S(\sigma, t) = f_1(\sigma) + f_2(t). \tag{13}$$

Now using (6) we find S:

$$vf_1' = -\dot f_2 = \text{const} = c \quad \Rightarrow$$
$$\Rightarrow \quad S' = \frac{c}{v}, \quad S = c\left(\int \frac{\mathrm{d}\sigma}{v(\sigma)} - t\right). \quad (14)$$

This relation between the material and spatial coordinates at steady motions of strings was established earlier by Nordenholz and O'Reilly (1995), and was applied in the analysis of steady operation of belt drives by Rubin (2000). From (11) we find the "mass flow rate" $mv = \rho c = \text{const}$.

The length of the belt in the reference configuration L equals to the length of the contour, and the variation of σ in the range from 0 to $L \equiv \sigma_4$ answers to the growth of s from 0 to L. The conditions $S(0) = 0$, $S(L) = L$ determine the constant c (this is the "condition of compatibility" in the terminology of Rubin (2000)).

The strain and the tension force can now be expressed through the field of velocity v:

$$\varepsilon = \frac{v}{c} - 1, \quad Q = Q_0 + b\left(\frac{v}{c} - 1\right). \quad (15)$$

The tangential projection of the balance equations in (10) leads to

$$\tilde q_\tau = mvv' - Q' = \rho c v' - Q'. \quad (16)$$

At a straight free span $\boldsymbol{q} = 0$, and from (16) follows

$$\rho c v - Q = \text{const} \quad \Rightarrow \quad v = \text{const} \quad (17)$$

as Q depends on v according to (15). At the tight span we have

$$v = v_+, \quad Q(v_+) = Q_+, \quad (18)$$

and at the slack one

$$v = v_-, \quad Q(v_-) = Q_-, \quad (19)$$

see Fig. 1.

At steady motion the moment at the driven pulley can be related to the velocities at the free spans. Substituting (16) in (12) and integrating, we obtain

$$M_B = k_B^{-1}\left((Q_+ - \rho c v_+) - (Q_- - \rho c v_-)\right). \quad (20)$$

At the pulleys we assume perfect contact:

$$v = \text{const} \quad \Rightarrow \quad Q = \text{const} \quad \Rightarrow \quad q_\tau = 0. \quad (21)$$

The seeming contradiction between (12), (20) and (21) is resolved by admitting discontinuities and corresponding concentrated forces at the points $\sigma = \sigma_i$: only the "outermost" zones on the pulleys are loaded. For the loading moment we get

$$M_B = -k_B^{-1}(F_2 + F_3),$$
$$F_i = [\rho c v - Q]_i = [mv^2 - Q]_i,$$
$$[\dots]_i \equiv \dots|_{\sigma=\sigma_i+0} - \dots|_{\sigma=\sigma_i-0}. \quad (22)$$

According to (16), the concentrated forces result from the jumps of the tension force and of the velocity in the corresponding points; see Irschik (2007) for a discussion.

Traditional treatment of the creep model (Reynolds, 1874; Rubin, 2000) assumes that the belt is contracting near the point σ_1, where it leaves the driving pulley A, and extending near the point σ_3, where it leaves the driven one B. For a friction belt drive a continuity condition needs to be imposed in the points σ_2 and σ_4, where the belt hits the pulleys. Indeed, according to the idealized model of contact the particles of the belt adhere to the surface of the pulleys at these points, and any jump here would have been transported further. Thus we conclude that in a steady regime the field $v(\sigma)$ is piecewise constant with two points of discontinuity σ_1 and σ_3. The velocities at the free spans coincide with the velocities of the surfaces of the pulleys:

$$v_+ = v_A = \omega_A k_A^{-1}, \quad v_- = v_B = \omega_B k_B^{-1}. \quad (23)$$

To simplify the subsequent analysis, from now on we assume the drive to be symmetric with

$$k_A = k_B = k. \quad (24)$$

Then from the compatibility condition (14) we find

$$\int_0^L \frac{c}{v}\,\mathrm{d}\sigma = L \quad \Rightarrow \quad \frac{1}{v_+} + \frac{1}{v_-} = \frac{2}{c}. \quad (25)$$

The working regime is determined by the ratio between the velocities at the tight and at the slack sides

$$\eta = \frac{v_+}{v_-} \ge 1, \quad v_+ = \frac{1}{2}c(1+\eta), \quad v_- = \frac{1}{2}c(1+\eta^{-1}), \quad (26)$$

and for the moments at the pulleys we find

$$M_B = -M_A = \frac{1}{2}k^{-1}(\eta - \eta^{-1})(b - \rho c^2). \quad (27)$$

The coefficient of efficiency of the drive is

$$-\frac{M_B\omega_B}{M_A\omega_A} = \frac{v_-}{v_+} = \frac{1}{\eta} \le 1; \quad (28)$$

more power is lost at higher transmitted moments.

In the technical literature it is commonly assumed that the mean value of the tension forces at the free spans equals to the pre-tension (see e.g. (Brar and Bansal, 2004; Niemann and Winter, 1986)). However, it is easy to see that

$$Q_+ + Q_- = 2Q_0 + \frac{1}{2}b(\eta + \eta^{-1} - 1) \ne 2Q_0, \quad (29)$$

and the difference grows at higher transmitted moments. Moreover, further additional analysis shows that the proposition does not generally hold for unsymmetric belt drives, when $k_A \ne k_B$.

4. TRANSIENT DYNAMICS: MATHEMATICAL MODEL

For both free spans with $\boldsymbol{q} = 0$ a single partial differential equation follows from the equalities (3)-(10):

$$\ddot S S'^2 + \dot S^2 S'' = 2S'\dot S\dot S' + \frac{b}{\rho}S''. \quad (30)$$

This wave equation can be classified as quasilinear, as in the material description for $\sigma(s,t)$ it is equivalent to

$$b\,\partial_s^2\sigma = \rho\,\partial_t^2\sigma. \quad (31)$$

The spatial form (30) is more advantageous as the boundary conditions are then placed at fixed points σ_i.

As discussed before (23), the particles of the belt immediately adhere to the pulley surface at the points σ_2 and σ_4. In these points we demand the velocity of the belt to be continuous, which leads to the boundary conditions for the equations of dynamics at the free spans (30):

$$\dot S + k^{-1}\omega_A\, S'|_{\sigma=\sigma_4} = 0,$$
$$\dot S + k^{-1}\omega_B\, S'|_{\sigma=\sigma_2} = 0. \quad (32)$$

Discussing the remaining conditions at the points σ_1 and σ_3, we focus our attention at the conditions for the driven pulley B. The equations for the driving pulley A are to be formulated by replacing the indices accordingly.

The solution is "transported" by the pulleys, and in the point σ_3 we have the material points from the point σ_2 with a certain delay:

$$S(\sigma_3, t) \equiv S_3(t) = S(\sigma_2, t - \tau_B(t)); \tag{33}$$

the particle with the material coordinate $S_3(t)$ came into contact with the pulley at the time instance $t-\tau_B(t)$. Since then, the pulley has rotated to the known angle:

$$\int\limits_{t-\tau_B(t)}^{t} \omega_B(\tilde{t})\,\mathrm{d}\tilde{t} = k^{-1}(\sigma_3 - \sigma_2) = \text{const}. \tag{34}$$

Differentiating with respect to time, we find the relation of the delay time to the angular velocity of the driven pulley:

$$\dot{\tau}_B(t) = 1 - \frac{\omega_B(t)}{\omega_B(t - \tau_B(t))}. \tag{35}$$

The problem is closed by the equations for the pulleys

$$I\dot{\omega}_A = M_A + M_A^{\text{ext}}, \quad I\dot{\omega}_B = M_B + M_B^{\text{ext}}. \tag{36}$$

The moments of inertia of the pulleys are denoted as I. External moments M_A^{ext}, M_B^{ext} are either given functions of time or may be governed by additional equations for a control loop. Computing the moments M_A and M_B, which act on the pulleys from the side of the belt, we again focus the attention at the driven one and substitute (10) in (12):

$$\begin{aligned} kM_B &= -\int\limits_{\sigma_2-0}^{\sigma_3+0} (mw_\tau - Q')\,\mathrm{d}\sigma = \\ &= Q|_{\sigma_2-0}^{\sigma_3+0} - \int\limits_{\sigma_2-0}^{\sigma_3+0} m\,(vv' + \dot{v})\,\mathrm{d}\sigma. \end{aligned} \tag{37}$$

The fields m, v and $\dot{v}$ have a discontinuity of the first kind at σ_3. "Concentrated" terms under the integral appear only due to v':

$$v = -\frac{\dot{S}}{S'}, \quad mvv' = \rho\left(\frac{\dot{S}\dot{S}'}{S'} - \frac{S''\dot{S}^2}{S'^2}\right); \tag{38}$$

$$\int\limits_{\sigma_3-0}^{\sigma_3+0} mvv'\,\mathrm{d}\sigma = -\rho\dot{S}_3^2 \int\limits_{\sigma_3-0}^{\sigma_3+0} \frac{S''\,\mathrm{d}\sigma}{S'^2} = \rho\dot{S}_3^2\left[(S')^{-1}\right]_3.$$

In the domain $\sigma_2 < \sigma < \sigma_3$ we have $\dot{v} = k^{-1}\dot{\omega}_B$, $v' = 0$, and the integral (37) results in the following three terms:

$$kM_B = Q|_{\sigma_2-0}^{\sigma_3+0} - \rho\dot{\omega}_B k^{-1}(S_3 - S_2) - \rho\dot{S}_3^2\left[(S')^{-1}\right]_3. \tag{39}$$

Here S_3 is again determined by the solution in the point 2 with a delay. In the expression for the jump of $(S')^{-1}$ the value at $\sigma_3 + 0$ is taken from the solution on the span 34, and the stretch at $\sigma_3 - 0$ is "transported" by the pulley:

$$(S')^{-1}\big|_{\sigma=\sigma_3-0,\ t=\tilde{t}} = (S')^{-1}\big|_{\sigma=\sigma_2,\ t=\tilde{t}-\tau_B(\tilde{t})}. \tag{40}$$

A simple interpretation can be given to all three terms at the right hand side of (39). The first term is just the moment due to the tension forces and is taken into account by all technical approaches. The second term represents additional inertia of the pulley due to the attached part of the belt. And the third non-trivial term is the reactive force at the point, where the velocity undergoes a jump.

It should be noted, that the expression (39) could be derived using relations of jump of mass and momentum known from the literature. Following Irschik (2007), we write the concentrated force, which acts on the belt in the point σ_3:

$$F_3 = [mv^2 - Q]_3 = \left[\rho S'\dot{S}^2(S')^{-2}\right]_3 - [Q]_3. \tag{41}$$

The force F_3 contributes to the moment M_B as in (22), and the jump of mv^2 evidently leads to the third term (reactive force) at the right hand side in (39).

5. NUMERICAL SCHEME

A central point of the simulation is the numerical solution of the partial differential equation (30). A system of ordinary differential equations, which can then be integrated over time using conventional methods, follows after a finite difference discretization with respect to the spatial coordinate σ (Pozrikidis, 2008; Vetyukov, 2014). We divide both free spans 12 and 34 into n segments and consider values

$$S^{(i)}(t) = S(\sigma^{(i)}, t) \tag{42}$$

of the unknown function at the equidistantly distributed nodes $\sigma^{(i)}$, $i = 0 \dots n$. The outmost nodes correspond to the end points of the domain, i.e.,

$$\sigma^{(0)} = \sigma_1, \quad \sigma^{(n)} = \sigma_2 \tag{43}$$

for the slack span and

$$\sigma^{(0)} = \sigma_3, \quad \sigma^{(n)} = \sigma_4 \tag{44}$$

for the tight span. We project the equation (30) onto the internal nodes of the grid $i = 1 \dots n-1$ by using central finite difference approximation for the spatial derivatives

$$\begin{aligned} (S')^{(i)} &\leftarrow \frac{S^{(i+1)} - S^{(i-1)}}{2h}, \\ (S'')^{(i)} &\leftarrow \frac{S^{(i+1)} - 2S^{(i)} + S^{(i-1)}}{h^2} \end{aligned} \tag{45}$$

and obtain $n-1$ ordinary differential equations for each free span; here $h = \sigma^{(i+1)} - \sigma^{(i)}$ is the step of the grid. There are n unknowns $S^{(1)}(t), \dots, S^{(n)}(t)$, as the values $S^{(0)}$ at the starting nodes of the grid σ_1 and σ_3 are directly available from the boundary conditions (33), which couples the solutions at both free spans. At the end points of the grid the particles immediately adhere to the surface of the pulleys, which means boundary conditions of the form

$$v(\sigma_2, t) = k^{-1}\omega_B(t), \quad v(\sigma_4, t) = k^{-1}\omega_A(t). \tag{46}$$

The first equality in (38) provides a relation between S and v, and for the stretch at the end point of the grid we use a left-sided finite difference approximation:

$$\left(\frac{1}{S'}\right)^{(n)} \leftarrow \frac{h}{S^{(n)} - S^{(n-1)}}. \tag{47}$$

The conditions (46) complete the set of differential equations for each free span.

Delay times τ_A and τ_B are additional unknowns in the problem with their own differential equations (35). Finally, for the angular velocities of the pulleys ω_A and ω_B we

integrate (36) over time. The resulting system of equations features $2(n-1)+2+2$ unknown functions of time.

According to (39) and (40), the moments M_A and M_B depend on the solution at the time instants $t-\tau_A$ and $t-\tau_B$ as well as (33) and (35). In the numerical simulations we need to solve a system of delay differential equations with variable delay times. An implementation in *Wolfram Mathematica* has been developed on the basis of the regular routine *NDSolve* for solving systems of ordinary differential equations. After each step of the time integration, the values S_2, $\dot S_2$, S_4, $\dot S_4$, ω_A and ω_B are saved into a data array for later use. The values of the unknowns at the time instants $t-\tau_A$ and $t-\tau_B$ at the right-hand sides of the differential equations are then interpolated over this array. Stretches $(S')^{-1}$ in (40) are expressed via $\dot S$ using the first equality in (38) as the velocities at the pulleys are known from (46).

It remains to notice, that the delays in the differential equations mean that the solution depends on the "pre-history" at the time period $t<0$; common initial conditions at the time instant $t=0$ are insufficient in the present case. Assuming the drive to be freely moving at a constant speed, such that $v=v_0$ at $t<0$, we find all necessary functions for this "pre-historic" period of time:

$$\begin{aligned}&\omega_A=\omega_B=kv_0,\\ &S=\sigma-v_0t,\quad \dot S=-v_0,\\ &\tau_A=\tau_B=\frac{\pi}{kv_0}.\end{aligned}\tag{48}$$

Starting from a moving state with $v_0>0$, we avoid difficulties with the infinite delay times in the beginning of the simulation.

6. RESULTS OF SIMULATIONS

The present model features dynamic effects, which are ignored by traditional approaches to modeling dynamics of belt drives. To make these effects prominent, we considered high rotation speeds and light pulleys. Choosing Young's modulus of the belt $E=10^8$, its volumetric material density $\rho_3=1200$ and its cross-section as a square with the size $a=5\times10^{-3}$ (all values are in SI units here and below), we compute its properties as follows:

$$b=Ea^2,\quad \rho=\rho_3a^2.\tag{49}$$

The radius of the pulleys and their moment of inertia are

$$k^{-1}=0.1,\quad I=20\rho\pi k^{-3},\tag{50}$$

such that I is 20 times larger than the moment of inertia of the part of the belt around the half of a pulley. The distance between the centers of the pulleys is $\sigma_2-\sigma_1=\sigma_4-\sigma_3=0.5$. At $t<0$, the structure is moving with the velocity $v_0=10$. Starting from the steady unloaded motion (48) at $t=0$, we apply an accelerating moment at the driving pulley $M_A^{\rm ext}=M=100$. After a certain period of time $\bar t$ we apply the same, but oppositely acting loading moment at the other pulley, such that

$$M_B^{\rm ext}=\begin{cases}0, & t<\bar t\\ -M, & t\ge\bar t.\end{cases}\tag{51}$$

Depending on the size of the time interval $\bar t$, the system accelerates to a certain speed level, and then keeps moving in a steady mode after the decay of the oscillations.

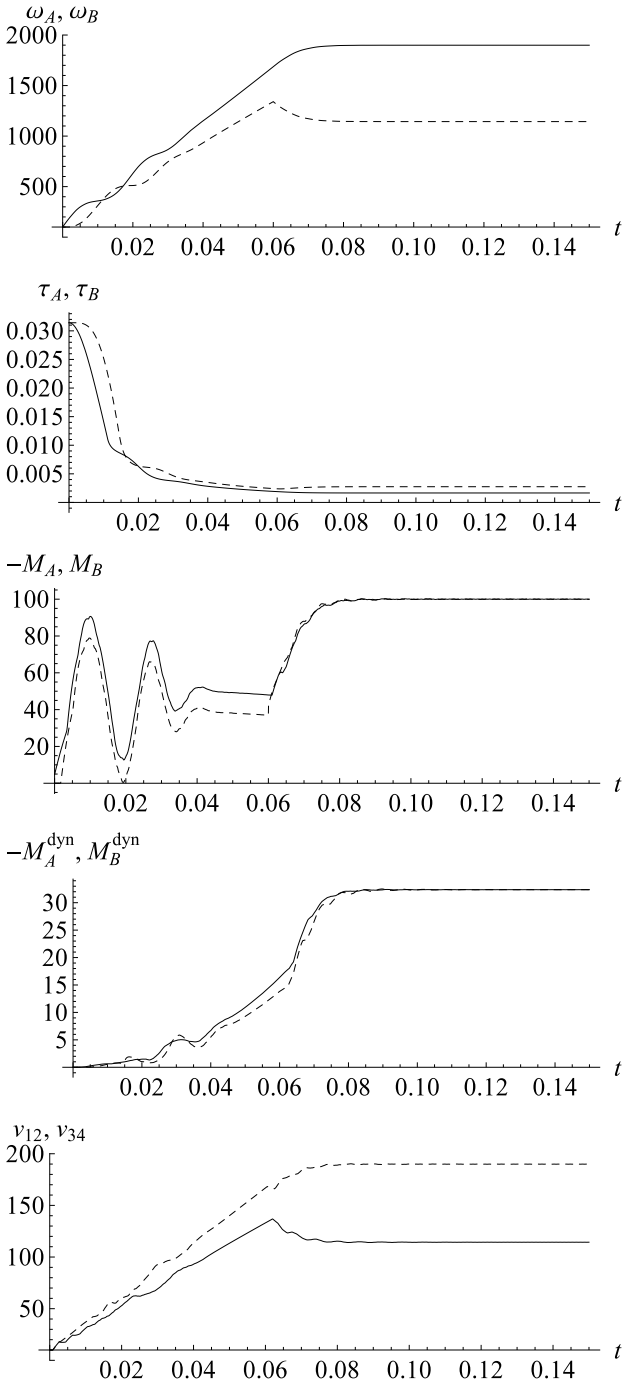

Fig. 2. Simulation results; the second variable indicated on the vertical axis is plotted with a dashed line

The structure is very light with short characteristic times, and we choose a value of the acceleration time $\bar t=0.06$ to make dynamic effects visible. The computed time histories of particularly interesting characteristics of the solution are presented in Fig. 2. We used $n=60$ segments of the finite difference discretization, as further refinement does not lead to noticeable changes in the presented results. The angular velocities of both pulleys grow during the acceleration stage, and after the drive is balanced by a loading moment at the driven pulley, the system quickly arrives at a steady regime of motion. The high ratio between the steady angular velocities $\eta=\omega_A/\omega_B\approx1.66$

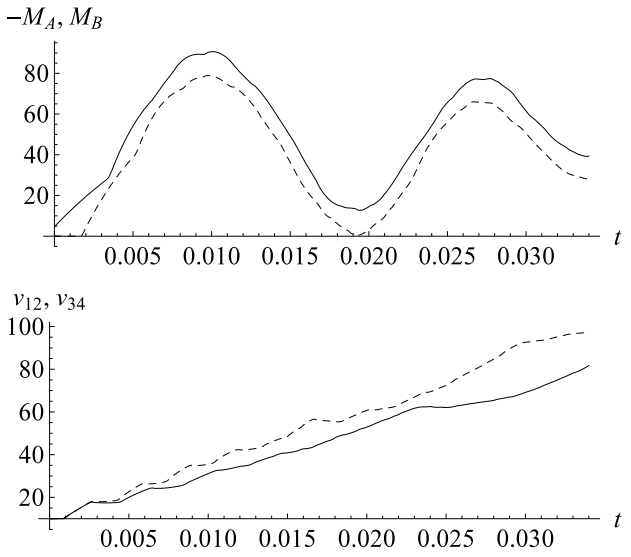

Fig. 3. Simulation results for the initial period of time

means high levels of deformations of the belt, and indeed at the tight span we have strain $\varepsilon \approx 0.33$, while at the slack span $\varepsilon \approx -0.2$. Fast rotation of the pulleys leads to very short delay times $\tau_{A,B}$ at the steady regime, which is clear from (34). Rotational moments, which act on the pulleys from the side of the belt, are rapidly changing during the acceleration stage, and quickly reach the values $-M^{\rm ext}_{A,B} = \pm M$ at the steady regime. The dynamic part in the moments $M^{\rm dyn}_{A,B}$, which is determined by the last reactive term in (39), is playing an important role at the considered high level of speed. And finally, we compare the velocities of the belt at the middle points of both free spans v_{12} and v_{34}. Their steady values are in perfect agreement with the analytical expression for the moments at the pulleys (27), while the constant $c \approx 142.8$ follows from (26). During the acceleration stage, the velocity varies linearly along the free spans, and at $t = \bar{t}$ the difference between the two ends is approximately 2%. It remains to notice, that the reached velocities are not too far below the critical value $\sqrt{b/\rho} \approx 288.7$, at which the physical transport speed equals to the wave speed and the solution of the transport problem undergoes a divergence instability (Wickert and Mote, 1990). Indeed, increasing $\bar{t}$ we observed "exploding" solutions as soon as the theoretically predicted critical speed level was exceeded.

In Fig. 3 we have shown the same results for the initial short period of time, such that the starting stage of the motion can be analyzed. The moment at the driven pulley appears after it is reached by a wave travelling through the free spans. The middle points of the free spans react to the applied driving moment after a two times shorter period of time, and several waves travelling across the belt can clearly be seen.

Concluding, we note that particular non-stationary regimes of motion (steady acceleration, harmonic response in the vicinity of a steady motion) may be studied analytically with the help of perturbation methods. Along with the presented numerical scheme, they shall provide a solid basis for testing the strategies of automatic control for belt drives at high and rapidly changing speeds.

REFERENCES

Antman, S. (1995). *Nonlinear problems of elasticity*. Springer, New York.

Bechtel, S., Vohra, S., Jacob, K., and Carlson, C. (2000). The stretching and slipping of belts and fibers on pulleys. *ASME Journal of Applied Mechanics*, 67, 197–206.

Brar, J. and Bansal, R. (2004). *A Text Book of Theory of Machines*. Laxmi publications, New Delhi.

Eliseev, V. and Vetyukov, Y. (2012). Effects of deformation in the dynamics of belt drive. *Acta Mechanica*, 223, 1657–1667.

Eliseev, V. (2009). A model of elastic string for transmissions with flexible coupling (in Russian). *Scientific and technical bulletin of St. Petersburg State Polytechnical University*, 84, 192–195.

Irschik, H. (2007). On rational treatments of the general laws of balance and jump, with emphasis on configurational formulations. *Acta Mechanica*, 194, 11–32.

Kim, D., Leamy, M., and Ferri, A. (2011). Dynamic modeling and stability analysis of flat belt drives using an elastic/perfectly plastic friction law. *ASME Journal of Dynamic Systems, Measurement, and Control*, 133, 1–10.

Kong, L. and Parker, R. (2005). Steady mechanics of belt-pulley systems. *ASME Journal of Applied Mechanics*, 72, 25–34.

Leamy, M. (2005). On a perturbation method for the analysis of unsteady belt-drive operation. *ASME Journal of Applied Mechanics*, 72(4), 570–580.

Morimoto, T. and Iizuka, H. (2012). Rolling contact between a rubber ring and rigid cylinders: Mechanics of rubber belts. *International Journal of Mechanical Sciences*, 54, 234–240.

Niemann, G. and Winter, H. (1986). *Maschinenelemente (in German)*, volume III. Springer, 2 edition.

Nordenholz, T. and O'Reilly, O. (1995). On kinematical conditions for steady motions of strings and rods. *ASME Journal of Applied Mechanics*, 62, 820–822.

Pozrikidis, C. (2008). *Numerical Computation in Science and Engineering*. Oxford University Press, 2nd edition.

Reynolds, O. (1874). On the efficiency of belts or straps as communicators of work. *The Engineer*, 38, 396.

Rubin, M. (2000). An exact solution for steady motion of an extensible belt in multipulley belt drive systems. *Journal of Mechanical Design*, 122, 311–316.

Stolarski, T.A. (1990). *Tribology in Machine Design*. Butterworth-Heinemann, Oxford.

Vetyukov, Y. (2014). *Nonlinear Mechanics of Thin-Walled Structures. Asymptotics, Direct Approach and Numerical Analysis*. Springer, Vienna.

Vetyukov, Y. and Eliseev, V. (2014). The model of a deformable string with discontinuities at spatial description in the dynamics of a belt drive. In H. Irschik, M. Krommer, and A. Belyaev (eds.), *Mechanics and Model-Based Control of Advanced Engineering Systems*, 275–283. Springer, Vienna.

Wickert, J. and Mote, C. (1990). Classical vibration analysis of axially moving continua. *Journal of Applied Mechanics*, 57(3), 738–744.